

## Improved formulation for a structure-dependent integration method

Shuenn-Yih Chang\*, Tsui-Huang Wu<sup>a</sup> and Ngoc-Cuong Tran<sup>a</sup>

*Department of Civil Engineering, National Taipei University of Technology,  
NTUT Box 2653, Taipei 106, Taiwan, Republic of China*

*(Received October 15, 2015, Revised July 18, 2016, Accepted July 19, 2016)*

**Abstract.** Structure-dependent integration methods seem promising for structural dynamics applications since they can integrate unconditional stability and explicit formulation together, which can enable the integration methods to save many computational efforts when compared to an implicit method. A newly developed structure-dependent integration method can inherit such numerical properties. However, an unusual overshooting behavior might be experienced as it is used to compute a forced vibration response. The root cause of this inaccuracy is thoroughly explored herein. In addition, a scheme is proposed to modify this family method to overcome this unusual overshooting behavior. In fact, two improved formulations are proposed by adjusting the difference equations. As a result, it is verified that the two improved formulations of the integration methods can effectively overcome the difficulty arising from the inaccurate integration of the steady-state response of a high frequency mode.

**Keywords:** overshoot; forced vibration response; local truncation error; high frequency modes; structure-dependent integration method

---

### 1. Introduction

A new family of structure-dependent integration methods has been successfully developed for structural dynamics (Chang 2014a). In general, the formulation of this family method is drastically different from the previously published structure-dependent integration methods (Chang 2002, 2007, 2009, 2010, 2014b, 2015, Gui *et al.* 2004, Kolay and Ricles 2004). In fact, both the two difference equations are structure dependent for the new family method. Whereas, for the previously published methods only the difference equation for displacement increment is structure dependent. It has been shown that the new family method can have favorable numerical properties, such as the explicit formulation, unconditional stability, no overshooting in the early free vibration response and second order accuracy. Notice that an explicit formulation implies that there is no nonlinear iterations per time step. Hence, many computational efforts can be saved when compared to implicit methods (Newmark 1959, Hilber *et al.* 1977, Wood *et al.* 1981, Chung

---

\*Corresponding author, Professor, E-mail: [changsy@ntut.edu.tw](mailto:changsy@ntut.edu.tw)

<sup>a</sup>Graduate Student

and Hulbert 1993, Zhou and Tamma 2006, Krenk 2008, Rezaiee-Pajand and Sarafrazi 2010, Bathe and Noh 2012, Gao, *et al.* 2012, Hadianfard 2012, Alamatian 2013). The unconditional stability of an integration method implies that the step size can be selected based on accuracy consideration only and there is no constraint on step size. As a result, the integration of the unconditional stability and explicit formulation together makes the new family method very computationally efficient.

In 1972, Goudreau and Taylor found an overshoot in the Wilson- $\theta$  method. This overshoot occurs in the early free vibration response and it will be diminished after a certain time. The cause of this overshoot has been well explored by Hilber and Hughes (1978). It was concluded that the long-term behavior of the displacement response is dominated by the spectral properties of the amplification matrix while the short-term potential for overshoot is determined by all the entries of the amplification matrix. Another unusual overshooting behavior in displacement response may also experience in a pseudodynamic test due to a displacement control error occurred in each time step (Shing and Mahin 1987, Shing and Manivannan 1990, Chang 2002, Bonelli and Bursi 2004). In the near recent, Bathe and Noh (2012) showed that an overshoot may occur in either velocity or acceleration response for high frequency modes for using the Newmark family method while the method developed by them can eliminate this unusual overshoot although both methods exhibit no overshoot in displacement response. Although the new family method seems to be very promising in earthquake engineering and structural dynamics applications, an unusual overshooting behavior in the displacement response is unexpectedly found in the step-by-step solution of a system subject to an external force. Apparently, this overshooting behavior is different from the above-mentioned overshooting behaviors. Consequently, an exploration of this overshooting behavior for the new family method is needed.

In general, the basic analysis of an integration method based on a free vibration response is able to obtain the numerical properties. However, the effect from dynamic loading to response is generally neglected in this analysis although an accurate representation of the dynamic loading has been studied (Chang 2006). Hence, the use of a forced vibration response rather than a free vibration response to conduct the basic analysis of an integration method seems preferable. Among the many numerical properties of an integration method, it seems that only the local truncation error derived from a forced vibration response can provide the information regarding the accuracy of numerical solution affected by an applied external force. Consequently, in this study, the local truncation error of the new family method will be derived from a forced vibration response and it will be applied to explain the cause of the unusual overshooting behavior. In addition, an improved formulation of the new family method is proposed to overcome the adverse overshooting behavior. All the analytical results will be thoroughly confirmed by numerical examples.

## 2. Integration method

In general, the formulation of the recently published structure-dependent integration method (Chang 2014a) can be expressed

$$ma_{i+1} + cv_{i+1} + kd_{i+1} = f_{i+1}$$

$$v_{i+1} = v_i + \psi(\Delta t) a_i \quad (1)$$

$$d_{i+1} = d_i + (\Delta t)v_i + \psi(\Delta t)^2 a_i$$

where  $m$ ,  $c$  and  $k$  are the mass, viscous damping coefficient and stiffness, respectively; and  $d_{i+1}$ ,  $v_{i+1}$ ,  $a_{i+1}$  and  $f_{i+1}$  correspond to the displacement, velocity, acceleration and external force at the end of the  $(i+1)$ -th time step. In addition, the structure-dependent coefficient  $\psi$  is found to be

$$\psi = \frac{1}{1 + 2\gamma\zeta\Omega_0 + \beta\Omega_0^2} = \frac{m}{m + \gamma(\Delta t)c_0 + \beta(\Delta t)^2 k_0} \quad (2)$$

where  $\beta$  and  $\gamma$  are free parameters to control the numerical properties;  $\zeta$  is a viscous damping ratio and  $\Omega_0 = \omega_0(\Delta t)$ ;  $\omega_0 = \sqrt{k_0/m}$  is the natural frequency of the system determined from the initial stiffness of  $k_0$ . The use of  $\Omega_0 = \sqrt{k_0/m}(\Delta t)$  and  $c_0 = 2\zeta\omega_0 m$  to replace  $\zeta$  and  $\Omega_0$  by  $c_0$ ,  $k_0$  and  $\Delta t$  is very important to improve computational efficiency since it avoids the need to conduct an eigen-analysis, which is very time consuming for a matrix of a large order. Apparently, both the two difference equations are explicit and are structure dependent. This family method will be referred as Chang family method (CFM) herein for brevity. Notice that it has been shown in the reference (Chang 2014a) that CFM generally displays no overshooting behavior in the early free vibration response, such as that found in the Wilson- $\theta$  method. In this study, the overshooting behavior of CFM in the forced vibration response is addressed.

### 3. Local truncation error

A local truncation error for an integration method is often defined as the error committed in each time step by replacing the differential equation with its corresponding difference equation (Belytschko and Hughes 1983). In this study, the local truncation error for CFM is derived from a forced vibration response rather than a free vibration response.

As a result, the approximating difference equation for CFM with the presence of a dynamic loading can be obtained from Eq. (1) after eliminating velocities and accelerations and is

$$d_{i+1} - \left(2 - \frac{2\zeta\Omega_0 + \Omega_0^2}{D}\right) d_i + \left(1 - \frac{2\zeta\Omega_0}{D}\right) d_{i-1} - \frac{1}{mD} (\Delta t)^2 f_i = 0 \quad (3)$$

where  $D = 1 + 2\gamma\zeta\Omega_0 + \beta\Omega_0^2$ . Thus, after replacing the differential equation with its corresponding difference equation, the local truncation error for CFM is found to be

$$E = \frac{1}{(\Delta t)^2} \left[ u(t + \Delta t) - \left(2 - \frac{2\zeta\Omega_0 + \Omega_0^2}{D}\right) u(t) + \left(1 - \frac{2\zeta\Omega_0}{D}\right) u(t - \Delta t) \right] - \frac{1}{mD} f_i \quad (4)$$

Assuming that  $u(t)$  and  $f(t)$  are continuously differentiable up to any required order,  $u(t+\Delta t)$  and  $u(t-\Delta t)$  can be expanded into finite Taylor series at  $t$ . As a result, Eq. (4) becomes

$$E = \frac{1}{D} \xi \Omega_0 (\Delta t) \dot{u}_i + \frac{2\gamma-1}{D} \xi \Omega_0 \ddot{u}_i + \frac{\beta^{-\frac{1}{2}}}{D} \Omega_0^2 \left( \ddot{u}_i - \frac{1}{k_0} \ddot{f}_i \right) + \frac{\beta}{D} \Omega_0^2 \frac{1}{k_0} \ddot{f}_i + O[(\Delta t)^3] \quad (5)$$

It is manifested from this equation that for  $\gamma=1/2$  CFM generally has an order of accuracy 2 for either a zero or nonzero external force. This analytical result indicates that CFM will generally give an accurate solution for a forced vibration response. Hence, the cause of the unusual overshooting behavior obtained from CFM for a system subject to an external force must be further investigated.

#### 4. An inaccurate forced vibration response

It is apparent that the local truncation error derived from a forced vibration response cannot be directly applied to explain why an inaccurate forced vibration response might be obtained by using CFM since it is second order accurate for a nonzero external force. Consequently, an actual example is applied to demonstrate that an inaccurate forced vibration response might be achieved if CFM is used to calculate the response. An intensive study of this example and a further exploration of the local truncation error might reveal the root cause of the inaccurate forced vibration response.

A linear elastic 2-degree of freedom system subject to a given external force is considered in this numerical example. The equation of motion for the 2-DOF system can be simply written as

$$\begin{bmatrix} m_1 & 0 \\ 0 & m_2 \end{bmatrix} \begin{Bmatrix} \ddot{u}_1 \\ \ddot{u}_2 \end{Bmatrix} + \begin{bmatrix} k_1 + k_2 & -k_2 \\ -k_2 & k_2 \end{bmatrix} \begin{Bmatrix} u_1 \\ u_2 \end{Bmatrix} = \begin{Bmatrix} k_1 \sin(\bar{\omega}t) \\ 0 \end{Bmatrix} \quad (6)$$

where  $m_1, m_2, k_1, k_2$  and  $\bar{\omega}$  can be arbitrarily specified to simulate a system. As a result, the two natural frequencies  $\omega_1$  and  $\omega_2$  as well as their corresponding modal shapes  $\phi_1$  and  $\phi_2$  can be determined. The two modal shapes can be explicitly expressed as

$$\phi_1 = \begin{Bmatrix} 1 \\ a \end{Bmatrix}, \quad \phi_2 = \begin{Bmatrix} 1 \\ b \end{Bmatrix} \quad (7)$$

As a result, the analytical solution to Eq. (4) can be theoretically found to be

$$\begin{Bmatrix} u_1(t) \\ u_2(t) \end{Bmatrix} = \begin{Bmatrix} 1 \\ a \end{Bmatrix} \left\{ \frac{k_1}{K_1} \frac{1}{1-\beta_1^2} [\sin(\bar{\omega}t) - \beta_1 \sin(\omega_1 t)] \right\} + \begin{Bmatrix} 1 \\ b \end{Bmatrix} \left\{ \frac{k_1}{K_2} \frac{1}{1-\beta_2^2} [\sin(\bar{\omega}t) - \beta_2 \sin(\omega_2 t)] \right\} \quad (8)$$

where  $\beta_1 = \bar{\omega} / \omega_1$ ,  $\beta_2 = \bar{\omega} / \omega_2$ ,  $K_1 = \phi_1^T \mathbf{K} \phi_1$  and  $K_2 = \phi_2^T \mathbf{K} \phi_2$ , where  $\mathbf{K}$  represents the stiffness matrix in Eq. (4). In Eq. (8), each response contribution to  $u_1$  or  $u_2$  is independent of the external force. This is because that each term on the right hand side of Eq. (8) is linearly proportional to  $k_1$ .

In Eq. (7),  $a$  will become very large and  $b$  tends to zero if the two modes are widely separated. In this case, the applied external force vector is very similar to the second modal shape. This implies that the steady-state response of the second mode might be largely excited and will

Table 1 Comparisons of response contributions for three different systems

Syst- em	$\omega_1$	$\omega_2$	$a$	$b$	$u_1$				$u_2$			
					1 <sup>st</sup> mode		2 <sup>nd</sup> mode		1 <sup>st</sup> mode		2 <sup>nd</sup> mode	
					$\frac{k_1}{K_1} \frac{1}{1-\beta_1^2}$	$\frac{k_1}{K_1} \frac{-\beta_1}{1-\beta_1^2}$	$\frac{k_1}{K_2} \frac{1}{1-\beta_2^2}$	$\frac{k_1}{K_2} \frac{-\beta_2}{1-\beta_2^2}$	$\frac{k_1}{K_1} \frac{a}{1-\beta_1^2}$	$\frac{k_1}{K_1} \frac{-\beta_1 a}{1-\beta_1^2}$	$\frac{k_1}{K_2} \frac{b}{1-\beta_2^2}$	$\frac{k_1}{K_2} \frac{-\beta_2 b}{1-\beta_2^2}$
S-1	0.9493	3.3321	0.099	-3.13×10 <sup>-2</sup>	6.60×10 <sup>-1</sup>	1.40×10 <sup>-1</sup>	-8.37×10 <sup>-1</sup>	-3.16×10 <sup>-1</sup>	6.67×10 <sup>-1</sup>	-1.38×10 <sup>-1</sup>	8.29×10 <sup>-2</sup>	
S-2	1	10 <sup>2</sup>	10 <sup>4</sup>	-10 <sup>-4</sup>	-3.33×10 <sup>-5</sup>	6.67×10 <sup>-5</sup>	1	-2.00×10 <sup>-2</sup>	-3.33×10 <sup>-1</sup>	6.67×10 <sup>-1</sup>	-1.00×10 <sup>-4</sup>	2.00×10 <sup>-6</sup>
S-3	1	10 <sup>3</sup>	10 <sup>6</sup>	-10 <sup>-6</sup>	-3.33×10 <sup>-7</sup>	6.67×10 <sup>-7</sup>	1	-2.00×10 <sup>-3</sup>	-3.33×10 <sup>-1</sup>	6.67×10 <sup>-1</sup>	-1.00×10 <sup>-6</sup>	2.00×10 <sup>-9</sup>

Note:  $u_1 = \frac{k_1}{K_1} \frac{1}{1-\beta_1^2} [\sin(\bar{\omega}t) - \beta_1 \sin(\omega_1 t)] + \frac{k_1}{K_2} \frac{1}{1-\beta_2^2} [\sin(\bar{\omega}t) - \beta_2 \sin(\omega_2 t)]$   
 $u_2 = \frac{k_1}{K_1} \frac{a}{1-\beta_1^2} [\sin(\bar{\omega}t) - \beta_1 \sin(\omega_1 t)] + \frac{k_1}{K_2} \frac{b}{1-\beta_2^2} [\sin(\bar{\omega}t) - \beta_2 \sin(\omega_2 t)]$

significantly contribute to  $u_1$ . This case seems appropriate to study the accuracy of the integration of the steady-state response of a high frequency mode. In addition, this case can be considered as a model problem to represent the stiff and flexible parts of a much more complex system. In order to have different combinations of the two vibration modes for three systems, structural properties are specified to simulate the three systems. In fact, the following three systems are considered:

$$\text{S-1 } m_1 = m_2 = 1, k_1 = 10^1, k_2 = 1 \text{ and } \bar{\omega} = 2$$

$$\text{S-2 } m_1 = m_2 = 1, k_1 = 10^4, k_2 = 1 \text{ and } \bar{\omega} = 2$$

$$\text{S-3 } m_1 = m_2 = 1, k_1 = 10^6, k_2 = 1 \text{ and } \bar{\omega} = 2$$

In order to gain inside into each response contribution to the total displacement response of the three different systems, each modal response contribution factor is summarized in Table 1.

The separation of the two modes can be evaluated by the ratio of  $\omega_2/\omega_1$ . The ratio of  $\omega_2/\omega_1$  for S-1, S-2 and S-3 are found to be 3.51, 10<sup>2</sup> and 10<sup>3</sup> correspondingly. It is clearly that a large ratio of  $\omega_2/\omega_1$  implies that the two modes are widely separated. In addition, the value of  $a$  is increased with the increase of  $\omega_2/\omega_1$  and it approaches the value of  $(\omega_2/\omega_1)^2$  for S-2 and S-3. On the other hand, the absolute value of  $b$  decreases from a relatively small value 0.099 to zero with the increase of  $\omega_2/\omega_1$ . In fact, for S-2 and S-3, the  $b$  value is almost zero. Hence, the load pattern  $[k_1 \sin(\bar{\omega}t), 0]^T$ , which is given in Eq. (6) becomes the same as the second modal shape  $\phi_2 = [1, 0]^T$  for S-2 and S-3. This implies that the steady-state response of the second mode will be largely excited by this load pattern for a large ratio of  $\omega_2/\omega_1$ , such as S-2 and S-3. This can be confirmed by the modal response contribution factors as shown in Table 1, where  $u_1$  is totally dominated by the steady-state response of the second mode for S-2 and S-3. Since the response contribution from the second mode to  $u_2$  is very small, thus,  $u_2$  is still dominated by the modal response of the first mode for both S-2 and S-3. Notice that the second modal shape for S-1 is  $\phi_2 = [1, -0.099]^T$ , which is different from the load pattern  $[k_1 \sin(\bar{\omega}t), 0]^T$ . Hence, it is anticipated that both the two modes of S-1 will be considerably excited. This can be manifested from the second row of

Table 1, where each modal response contribution factor for S-1 have roughly the same order of magnitude due to a relatively small value of  $\omega_2/\omega_1$ . Hence, both the transient and steady-state responses of the two modes will considerably contribute to  $u_1$  and  $u_2$ .

In the following numerical illustrations, CFM will be applied to solve Eq. (6). Since a second order accuracy can be achieved for  $\gamma=1/2$ , thus it is adopted. Meanwhile, the cases of  $\beta=1/4$  and  $1/2$  are also considered. For brevity, CFM1 denotes the member of  $\beta=1/4$  and  $\gamma=1/2$  of CFM while the member of  $\beta=1/2$  and  $\gamma=1/2$  is denoted by CFM2. Notice that CFM2 can have an improved stability property for instantaneous stiffness hardening systems when compared to CFM1 (Chang 2014a). A time step of  $\Delta t=0.1$  sec is used to conduct time integration. This time step results in  $\Delta t/\bar{T}=0.032$ . This implies that the variation of the applied external force can be very accurately represented (Chang 2006). This time step also leads to  $\Delta t/T_1=0.015$  and  $\Delta t/T_2=0.053$  for S-1, where  $\bar{T}=2\pi/\bar{\omega}$ ,  $T_1=2\pi/\omega_1$  and  $T_2=2\pi/\omega_2$ . Thus, the two modes of S-1 can be reliably integrated. Similarly,  $\Delta t/T_1=0.016$  is found for both S-2 and S-3. Whereas,  $\Delta t/T_2=1.59$  is found for S-2 and  $\Delta t/T_2=15.92$  is found for S3. These values indicate that the first mode can be accurately integrated for S-2 and S-3 while a significant period distortion will be found in the second mode.

All the calculated results are shown in Fig. 1. In order to have a closer examination of the overshooting behavior of  $u_1$ , only the interval of 15 to 20 sec are plotted in Figs. 1(c) to 1(f). Notice that the displacement responses of  $u_2$  are not shown in this figure since the results obtained from CFM1 and CFM2 are always coincided with the exact solution. It is seen in Figs. 1(a) and 1(b) that both CFM1 and CFM2 provide very accurate solutions of  $u_1$  for S-1. This is mainly because that both modes of S-1 can be very accurately integrated. On the other hand, an overshooting behavior is found in the displacement response  $u_1$  for both S-2 and S-3 for either CFM1 or CFM2. Notice that an inaccurate result of  $u_1$  implies that the steady-state response of the second mode is not reliably integrated since  $u_1$  is entirely dominated by it, which is manifested from Table 1. This numerical example reveals that CFM might experience the difficulty arising from an inaccurate integration of the steady-state response of a high frequency mode. In addition, the overshooting behavior will become more significant with the increase of the natural frequency. This can be manifested from Fig. 1 and Table 1.

## 5. A deep investigation of local truncation error

Although the local truncation error of CFM as shown in Eq. (5) reveals that CFM can generally have a second order accuracy if  $\gamma=1/2$  is adopted for either a zero or nonzero external force. However, the illustrated example clearly shows that both CFM1 and CFM2 give an inaccurate result of  $u_1$  for S-2 and S-3, which is entirely dominated by the steady-state response of the second high frequency mode. On the other hand, both methods can provide an accurate solution of  $u_1$  for S-1, where the two low frequency modes considerably contribute to the total response. This strongly indicates that an inaccurate solution of the steady-state response might be experienced as the second mode is a relatively high frequency mode when compared to the first mode. Hence, a deep study of the local truncation error is needed for exploring the root cause of this inaccuracy.

Since a viscous damping ratio is generally small for real structure and  $\gamma=1/2$  is needed to have a second order accuracy, the local truncation error in Eq. (5) is generally dominated by the two terms of  $(\beta - \frac{1}{12})\Omega_0^2(\ddot{u}_i - \ddot{f}_i/k_0)/D$  and  $\beta\Omega_0^2\ddot{f}_i/(k_0D)$ . This implies that the dominant terms of

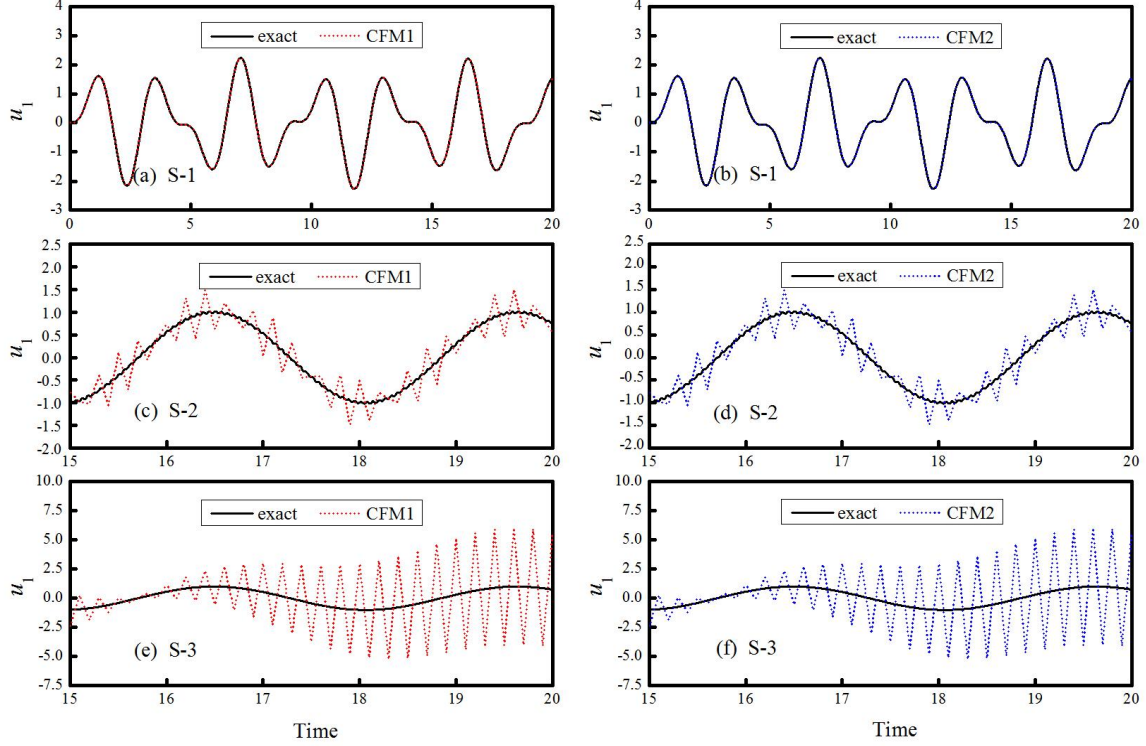


Fig. 1 Displacement response of  $u_1$  to a linear elastic 2-DOF system for CFM1 and CFM2

the local truncation error are quadratically proportional to the natural frequency  $\omega_0$  for either a free vibration response or a forced vibration response. Notice that the first term will reduce to be  $(\beta - \frac{1}{12})\Omega_0^2 \ddot{u}_i / D$  for a free vibration response. At first glance, it seems that the local truncation error derived from a forced vibration response is still unable to explain the cause of the difficulty arising from the inaccurate integration of the steady-state response of a high frequency mode. However, after a deep study of the term  $(\beta - \frac{1}{12})\Omega_0^2 (\ddot{u}_i - \ddot{f}_i / k_0) / D$ , it is found that it can be transformed into a new form through the governing equation of motion  $(\Delta t)^2 \ddot{u}_i + 2\xi\Omega_0(\Delta t)\dot{u}_i = \Omega_0^2(f_i / k_0 - u_i)$ . In this equation, the only term on the right hand side is quadratically proportional to  $\omega_0$ . Whereas, on the left hand side of this equation, the term  $2\xi\Omega_0(\Delta t)\dot{u}_i$  is linearly proportional to  $\omega_0$  and the term  $(\Delta t)^2 \ddot{u}_i$  is independent of  $\omega_0$ . Hence, the equation of motion can be considered as a transformation equation to reduce the order of the dependence on  $\omega_0$  for a local truncation error. As a result, after conducting the second derivative of the equation of motion, one can have

$$(\Delta t)^2 \dddot{u}_i + 2\xi\Omega_0(\Delta t)\ddot{u}_i = \Omega_0^2\left(\frac{1}{k_0}\dot{f}_i - \dot{u}_i\right) \quad (9)$$

Next, substituting this equation into Eq. (5), it becomes

$$E = \frac{1}{D} \xi \Omega_0 (\Delta t) \dot{u}_i + \frac{2\gamma-1}{D} \xi \Omega_0 \ddot{u}_i - \frac{\beta^{-\frac{1}{12}}}{D} [(\Delta t)^2 \dddot{u}_i + 2\xi \Omega_0 (\Delta t) \ddot{u}_i] + \frac{\beta}{D} \Omega_0^2 \frac{1}{k_0} \ddot{f}_i + O[(\Delta t)^3] \quad (10)$$

This equation indicates that for  $\gamma=1/2$  and zero viscous damping the dominant term of the local truncation error will be quadratically proportional to  $\omega_0$  for a high frequency mode. Consequently, it seems that the presence of the term  $\beta \Omega_0^2 \ddot{f}_i / (k_0 D)$  in the local truncation error is the root cause to an inaccurate integration of the steady-state response of a high frequency mode. It also indicates that there will be no such a problem for a low frequency mode in the forced vibration response. On the other hand, Eq. (10) reveals that no error term is quadratically proportional to  $\omega_0$  for a free vibration response and thus there will be no difficulty in the integration of the transient response of a high frequency mode.

## 6. Improved formulation to eliminate adverse term

It is manifested from Eq. (10) that the local truncation error for CFM can be reduced from the case of quadratically proportional to  $\omega_0$  to the case of linearly proportional to  $\omega_0$  if the term  $\beta \Omega_0^2 \ddot{f}_i / (k_0 D)$  is removed. Apparently, this term can be eliminated if an extra term  $-\beta \Omega_0^2 \ddot{f}_i / (k_0 D)$  is introduced into the local truncation error. It is natural to consider the possibility of modifying the general formulation of CFM so that an improved integration method can be achieved.

In order to automatically cancel out the adverse term of  $\beta \Omega_0^2 \ddot{f}_i / (k_0 D)$  in the local truncation error, an additional term is intentionally introduced into each original formulation of the difference equation. As a result, the two difference equations become

$$\begin{aligned} d_{i+1} &= d_i + (\Delta t) v_i + \psi (\Delta t)^2 a_i + \phi_{i+1} \\ v_{i+1} &= v_i + \psi (\Delta t) a_i + \theta_{i+1} \end{aligned} \quad (11)$$

where  $\phi_{i+1}$  and  $\theta_{i+1}$  will be appropriately determined. As a result, the local truncation error for the modified integration method is found to be

$$\begin{aligned} E &= \frac{1}{D} \xi \Omega_0 (\Delta t) \dot{u}_i + \frac{2\gamma-1}{D} \xi \Omega_0 \ddot{u}_i + \frac{\beta^{-\frac{1}{12}}}{D} \Omega_0^2 \ddot{u}_i + \frac{1}{D} \Omega_0^2 \frac{1}{k_0} \ddot{f}_i \\ &+ \frac{1}{(\Delta t)^2} \left[ \left( 1 - \frac{2\xi\Omega}{D} \right) \phi_i - \left( 1 - \frac{2\xi\Omega}{D} \right) \theta_i - \phi_{i+1} \right] + O[(\Delta t)^3] \end{aligned} \quad (12)$$

Based on this equations,  $\phi_{i+1}$  and  $\theta_{i+1}$  can be appropriately selected.

It is clear that the simple way to determine  $\phi_{i+1}$  and  $\theta_{i+1}$  is to apply Eq. (12) to remove the adverse term  $\beta \Omega_0^2 \ddot{f}_i / (k_0 D)$ . As a result, two combinations of  $\phi_{i+1}$  and  $\theta_{i+1}$  can be chosen to satisfy the requirement. The first combination of  $\phi_{i+1}$  and  $\theta_{i+1}$  can be determined by assuming that  $\theta_{i+1}=0$  for simplicity. As a result, they are found to be

$$\phi_{i+1} = \frac{\beta}{D} \frac{1}{m} (\Delta t)^2 (f_{i+1} - f_i) = \frac{\beta (\Delta t)^2 (f_{i+1} - f_i)}{m + \gamma (\Delta t) c_0 + \beta (\Delta t)^2 k_0}, \quad \theta_{i+1} = 0 \quad (13)$$

On the other hand, the second combination of  $\phi_{i+1}$  and  $\theta_{i+1}$  can be determined after assuming that  $\theta_{i+1} = \phi_{i+1}$ . Consequently,  $\phi_{i+1}$  and  $\theta_{i+1}$  are found to be

$$\phi_{i+1} = \frac{\beta}{D} \frac{1}{m} (\Delta t)^2 (f_{i+1} - 2f_i + f_{i-1}) = \frac{\beta (\Delta t)^2 (f_{i+1} - 2f_i + f_{i-1})}{m + \gamma (\Delta t) c_0 + \beta (\Delta t)^2 k_0}, \quad \theta_{i+1} = \phi_{i+1} \quad (14)$$

For brevity, the modified integration method with  $\phi_{i+1}$  and  $\theta_{i+1}$  defined in Eq. (13) is referred as MAA while that with  $\phi_{i+1}$  and  $\theta_{i+1}$  defined in Eq. (14) is referred as MAB. In general,  $\phi_{i+1}$  and  $\theta_{i+1}$  are basically different from the structure-dependent coefficient  $\psi$  since their numerators are functions of the external force increment although their denominators are the same as that of  $\psi$ . It is clear that  $\phi_{i+1}$  for MAA will involve the external force data for the current time step and the previous one step while both  $\phi_{i+1}$  and  $\theta_{i+1}$  for MAB involves that for the current time step and the previous two steps. Hence, MAA is simpler than for MAB. Notice that only the difference equation for displacement increment is modified by  $\phi_{i+1}$  for MAA while both the two difference equations are adjusted for MAB by  $\phi_{i+1}$  and  $\theta_{i+1}$ .

It is apparent that  $\phi_{i+1}$  and  $\theta_{i+1}$  will become zero for a free vibration case. Thus, the addition of  $\phi_{i+1}$  in the difference equation for displacement increment and that of  $\theta_{i+1}$  in the difference equation for velocity increment will not alter the basic numerical properties of CFM, such as the stability, numerical dissipation, relative period error and overshooting. Hence, there is no need to assess these basic numerical properties again. The only change of the numerical properties for either MAA or MAB is the local truncation error due to the modification of the difference equation for displacement increment and/or velocity increment when compared to CFM. As a result, after this modification of CFM, it is anticipated that the modified methods MAA and MAB can effectively overcome the unusual overshooting.

It might be of interest to consider the special case of the dynamic loading if it is a function of displacement. In the derivation of the local truncation error as shown in Eq. (4), it is required that  $f(t)$  is assumed to be continuously differentiable up to the required order. Hence, the second-order accuracy can be achieved if  $f(t)$  is continuously differentiable up to the second order.

## 7. Implementation for MAA

It is of need to conduct the numerical experiments to verify that the two modified integration methods can overcome the difficulty caused by the inaccurate solution of the steady-state response of a high frequency mode. For this purpose, the implementation details of MAA for a multiple degree of freedom system is sketched next.

In general, for a multiple degree of freedom system, the formulation of MAA can be simply expressed as

$$\begin{aligned} \mathbf{M} \mathbf{a}_{i+1} + \mathbf{C} \mathbf{v}_{i+1} + \mathbf{K} \mathbf{d}_{i+1} &= \mathbf{f}_{i+1} \\ \mathbf{d}_{i+1} &= \mathbf{d}_i + (\Delta t) \mathbf{v}_i + \Psi (\Delta t)^2 \mathbf{a}_i + \Phi_{i+1} \end{aligned}$$

$$\mathbf{v}_{i+1} = \mathbf{v}_i + \Psi(\Delta t)\mathbf{a}_i \quad (15)$$

It is clear that  $\Psi$  and  $\Phi_{i+1}$  are the coefficient matrices for a multiple degree of freedom system in correspondence to the scalar coefficients of  $\psi$  and  $\phi_{i+1}$  for a single degree of freedom system. As a result,  $\Psi$  and  $\Phi_{i+1}$  are found to be

$$\begin{aligned} \Psi &= \mathbf{D}^{-1}\mathbf{M} \\ \Phi_{i+1} &= \mathbf{D}^{-1}\beta(\Delta t)^2(\mathbf{f}_{i+1} - \mathbf{f}_i) \end{aligned} \quad (16)$$

where  $\mathbf{D} = \mathbf{M} + \gamma(\Delta t)\mathbf{C}_0 + \beta(\Delta t)^2\mathbf{K}_0$ . Notice that  $\mathbf{K}_0$  is an initial stiffness matrix. In general, the stiffness matrix  $\mathbf{K}$  in the first line of Eq. (15) is generally different from  $\mathbf{K}_0$  for a nonlinear system. Similarly,  $\mathbf{C}_0$  is an initial viscous damping matrix and  $\mathbf{C}$  may be different from  $\mathbf{C}_0$  for a nonlinear system. In practice,  $\mathbf{C} = \mathbf{C}_0$  might be adopted for a complete integration procedure.

After conducting the time integration for the  $i$ -th time step, the displacement vector  $\mathbf{d}_{i+1}$  at the end of the  $(i+1)$ -th time step can be computed by using the second line of Eq. (15) and is numerically equivalent to

$$\mathbf{D}[\mathbf{d}_{i+1} - \mathbf{d}_i - (\Delta t)\mathbf{v}_i] = (\Delta t)^2[\mathbf{a}_i + \beta(\mathbf{f}_{i+1} - \mathbf{f}_i)] \quad (17)$$

Next, the velocity vector can be calculated by using the third line of Eq. (15) and is equivalent to solve the following equations

$$\mathbf{D}(\mathbf{v}_{i+1} - \mathbf{v}_i) = \mathbf{M}(\Delta t)\mathbf{a}_i \quad (18)$$

Finally, the acceleration vector can be determined by using the equation of motion and is

$$\mathbf{M}\mathbf{a}_{i+1} = \mathbf{f}_{i+1} - \mathbf{C}\mathbf{v}_{i+1} - \mathbf{r}_{i+1} \quad (19)$$

where  $\mathbf{r}_{i+1}$  is often used to replace  $\mathbf{K}\mathbf{d}_{i+1}$  for a nonlinear system. In general, the Gauss elimination method, which usually consists of a triangulation and a substitution for each time step, can be used to solve Eqs. (17), (18) and (19). Notice that the triangulation of  $\mathbf{D}$  and  $\mathbf{M}$  is required to be conducted only once since they will remain invariant for a whole integration procedure. In addition, there is no need to triangulate  $\mathbf{M}$  if it is a diagonal matrix.

Notice that a distinct starting procedure might be needed for MAB since  $\Phi_{i+1}$  and  $\theta_{i+1}$  are functions of the current step data and the two previous step data. It is apparent that MAA can be simply adopted to start the computing procedure.

## 8. Numerical confirmations

The obtained analytical results strongly indicate that the modified integration methods MAA and MAB can overcome the difficulty arising from the inaccurate integration of the steady-state response of a high frequency mode. This is because that their local truncation errors can be reduced from quadratically proportional to natural frequency to linearly proportional to natural

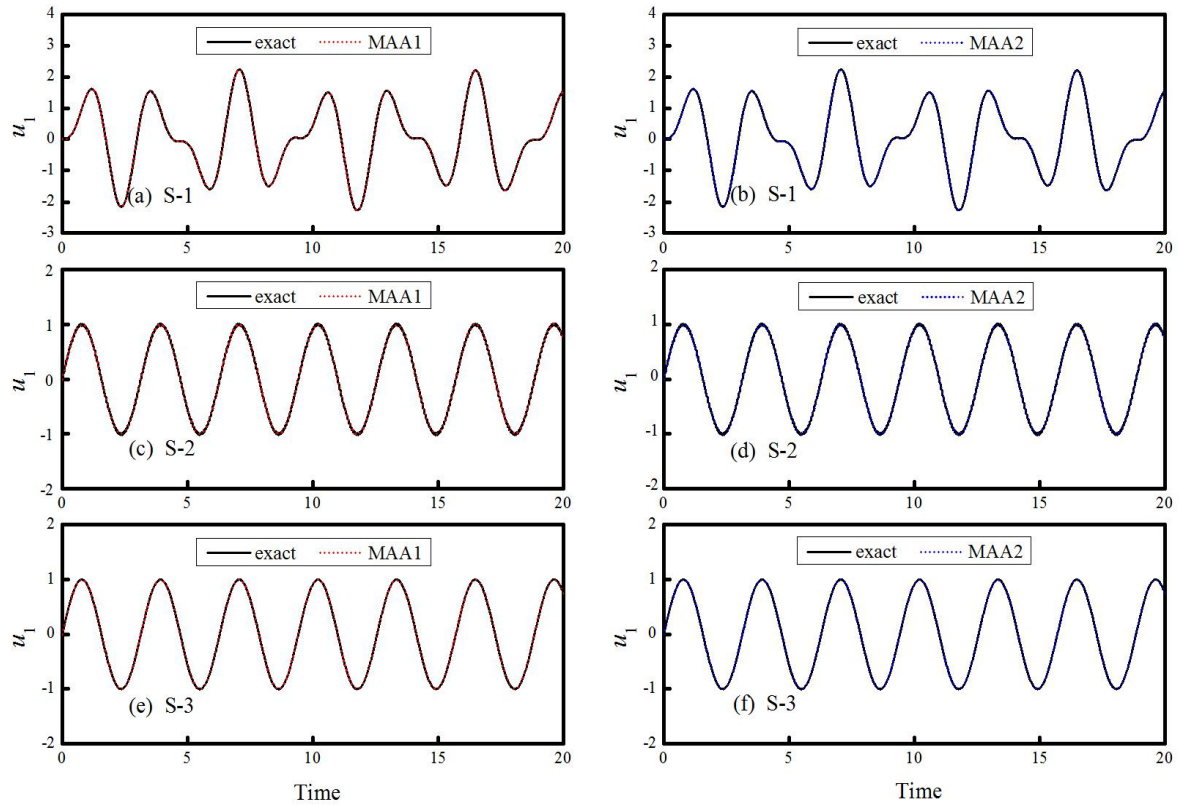


Fig. 2 Displacement response of  $u_1$  to a linear elastic 2-DOF system for MAA1 and MAA2

frequency or even to independent of natural frequency. Hence, it is of interest to confirm the performance of the two modified integration methods by numerical example. For this purpose, the illustrated problem, as shown in Eq. (6), is solved by MAA and MAB again and the numerical results are plotted in Figs. 2 and 3 respectively. For brevity, MAA1 is used to represent the member of MAA with  $\beta=1/4$  and  $\gamma=1/2$  while the member of  $\beta=1/2$  and  $\gamma=1/2$  for MAA is represented by MAA2. Similarly, MAB1 and MAB2 are named accordingly.

In Fig. 2, the numerical results, either calculated by MAA1 or MAA2, are almost coincided together with the exact solutions for all the three system. Notice that the time step of  $\Delta t=0.1$  sec is also adopted to conduct all the computations. Almost the same phenomenon is also found in Fig. 3, where MAB1 and MAB2 are employed to carry out the time integration with  $\Delta t=0.1$  sec. These results attest to that the difficulty caused by the inaccurate integration of the steady-state response of a high frequency mode can be entirely eliminated by the modified integration methods. This implies that the modification of the difference equation based on the local truncation error derived from a forced vibration response can lead to an improved formulation of CFM. As a result, MAA and MAB are the two improved formulations of CFM and they can effectively overcome the difficulty arising from the inaccurate integration of the steady-state response of a high frequency mode.

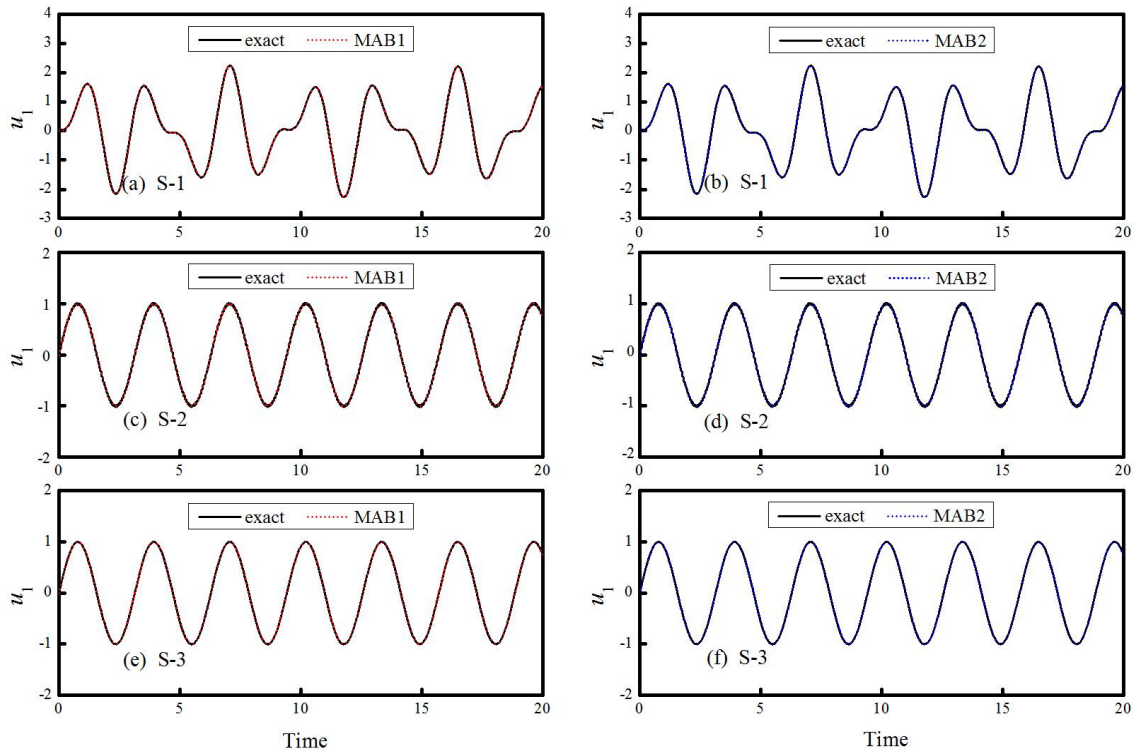


Fig. 3 Displacement response of  $u_1$  to a linear elastic 2-DOF system for MAB1 and MAB2

## 9. Conclusions

In this investigation, an unusual overshooting behavior is found in the step-by-step solution of a system subject to an external force if the newly developed structure-dependent integration method is applied. It is analytically shown that this family method will lead to an inaccurate integration of the steady-state response of a high frequency mode. In order to overcome the difficulty, an improved scheme is proposed to adjust the difference equations based on the local truncation error derived from a forced vibration response. As a result, two improved formulations of the newly developed family method are proposed. This scheme is to simply introduce an extra term, which is a function of the external force increment, into the difference equation for displacement increment and/or for velocity increment. The two improved formulations of the integration methods are verified by a numerical example and the results reveal that they can effectively overcome the difficulty caused by the inaccurate integration of the steady-state response of a high frequency mode.

## Acknowledgements

The author is grateful to acknowledge that this study is financially supported by the National Science Council, Taiwan, R.O.C., under Grant No. NSC-100-2211-E-027-012.

## References

- Alamatian, J. (2013), “New implicit higher order time integration for dynamic analysis”, *Structural Engineering and Mechanics, An International Journal*, **48**(5), 711-736.
- Bathe, K.J. and Noh, G. (2012), “Insight into an implicit time integration scheme for structural dynamics”, *Computers and Structures*, **98-99**, 1–6.
- Belytschko, T. and Hughes, T.J.R. (1983), *Computational Methods for Transient Analysis*, Elsevier Science Publishers B.V., North-Holland, Amsterdam.
- Bonelli, A. and Bursi, O.S. (2004), “Generalized- methods for seismic structural testing”, *Earthquake Engineering and Structural Dynamics*, **33**, 1067–1102
- Chang, S.Y. (2002), “Explicit pseudodynamic algorithm with unconditional stability”, *Journal of Engineering Mechanics, ASCE*, **128**(9), 935-947.
- Chang, S.Y. (2006), “Accurate representation of external force in time history analysis”, *Journal of Engineering Mechanics, ASCE*, **132**(1), 34-45.
- Chang, S.Y. (2007), “Improved explicit method for structural dynamics”, *Journal of Engineering Mechanics, ASCE*, **133**(7), 748-760.
- Chang, S.Y. (2009), “An explicit method with improved stability property”, *International Journal for Numerical Method in Engineering*, **77**(8), 1100-1120.
- Chang, S.Y. (2010), “A new family of explicit method for linear structural dynamics”, *Computers & Structures*, **88**(11-12), 755-772.
- Chang, S.Y. (2014a), “Family of structure-dependent explicit methods for structural dynamics”, *Journal of Engineering Mechanics, ASCE*, **140**(6), 06014005.
- Chang, S.Y. (2014b), “Numerical dissipation for explicit, unconditionally stable time integration methods”, *Earthquakes and Structures, An International Journal*, **7**(2), 157-176.
- Chang, S.Y., Wu, T.H. and Tran, N.C. (2015), “A family of dissipative structure-dependent integration methods”, *Structural Engineering and Mechanics, An International Journal*, **55**(4), 815-837.
- Chung, J. and Hulbert, G.M. (1993), “A time integration algorithm for structural dynamics with improved numerical dissipation: the generalized  $-\alpha$  method”, *Journal of Applied Mechanics*, **60**(6), 371-375.
- Gao, Q., Wu, F., Zhang, H.W., Zhong, W.X., Howson W.P. and Williams, F.W. (2012), “A fast precise integration method for structural dynamics problems”, *Structural Engineering and Mechanics, An International Journal*, **43**(1), 1-13.
- Goudreau, G.L. and Taylor, R.L. (1972), “Evaluation of numerical integration methods in elasto- dynamics”, *Computer Methods in Applied Mechanics and Engineering*, **2**, 69-97.
- Gui, Y., Wang, J.T., Jin, F., Chen, C. and Zhou, M.X. (2014), “Development of a family of explicit algorithms for structural dynamics with unconditional stability”, *Nonlinear Dynamics*, **77**(4), 1157-1170.
- Hadianfard, M.A. (2012), “Using integrated displacement method to time-history analysis of steel frames with nonlinear flexible connections”, *Structural Engineering and Mechanics, An International Journal*, **41**(5), 675-689.
- Hilber, H.M., Hughes, T.J.R. and Taylor, R.L. (1977), “Improved numerical dissipation for time integration algorithms in structural dynamics”, *Earthquake Engineering and Structural Dynamics*, **5**, 283-292.
- Hilber, H.M. and Hughes, T.J.R. (1978), “Collocation, dissipation, and ‘overshoot’ for time integration schemes in structural dynamics”, *Earthquake Engineering and Structural Dynamics*, **6**, 99-118.
- Kolay, C. and Ricles, J.M. (2014), “Development of a family of unconditionally stable explicit direct integration algorithms with controllable numerical energy dissipation”, *Earthquake Engineering and Structural Dynamics*; **43**, 1361–1380.
- Krenk, S. (2008), “Extended state-space time integration with high-frequency energy dissipation”, *International Journal for Numerical Methods in Engineering*, **73**, 1767- 1787.
- Newmark, N.M. (1959), “A method of computation for structural dynamics”, *Journal of Engineering Mechanics Division, ASCE*, **85**, 67-94.

- Rezaiee-Pajand, M., Sarafrazi, S.R., (2010), “A mixed and multi-step higher-order implicit time integration family”, *Journal of Mechanical Engineering Science*, **224**, 2097-2108.
- Shing, P.B. and Mahin, S.A. (1987), “Cumulative experimental errors in pseudodynamic tests”, *Journal of Engineering Mechanics*, ASCE, **15**, 409-424.
- Shing, P.B. and Maninannan T. (1990), “On the accuracy of an implicit algorithm for pseudo- dynamic tests”, *Journal of Engineering Mechanics*, ASCE, **19**, 631-651.
- Wood, W.L., Bossak, M. and Zienkiewicz, O.C. (1981), “An alpha modification of Newmark’s method”, *International Journal for Numerical Methods in Engineering*, **15**, 1562- 1566.
- Zhou, X. and Tamma, K.K. (2006), “Algorithms by design with illustrations to solid and structural mechanics/dynamics”, *International Journal for Numerical Methods in Engineering*, **66**, 1738–1790.